ABSTRACT

HUTCHINSON, SHANE ROBERT. Power Supply, Protection, and Harmonic Analysis for an Electric Vehicle Charging System in a Large Parking Deck. (Under the direction of Mesut E. Baran.)

This thesis presents a power delivery architecture for an Electric Vehicle (EV) and Plug-in Hybrid Electric Vehicle (PHEV) charging system to be implemented in a parking deck for consumer use.

The main design issues for this topic are covered, including the characterization of the PHEV and EV load using simulations, the layout of the power supply circuit, the sizing of cables and transformers, and electrical protection.

The National Electrical code is used to size the equipment, following the guidelines of the IEEE Recommended Practice for Electric Power Systems in Commercial Buildings. The transformer is sized by a statistical analysis with the Monte Carlo method of the expected power by looking at the arrival times and initial states of charge of the vehicle batteries connected to the system.

Included in this design is a current harmonic analysis of the HEV Toyota Prius with a Hymotion plug-in aftermarket kit and the Progress Energy Ford Escape PHEV. The NC State ATEC charger is also analyzed in software to get a comparison of the charger topologies. The harmonic current analysis and its effects on the transformer rating are discussed. The harmonic phase cancellation phenomenon is studied for the charging system, where current harmonics for multiple chargers connected to the same system are phase shifted from one another, resulting in a lesser value for the total distortion than the strict arithmetic sum of the harmonic current

magnitudes. Final results are obtained by using the Monte Carlo method to apply a derating factor for the transformer in accordance with the IEEE C57.110 Standard.

Power Supply, Protection, and Harmonic Analysis for an Electric Vehicle Charging System in a Large Parking Deck

by
Shane Hutchinson

A thesis submitted to the Graduate Faculty of
North Carolina State University
in partial fulfillment of the
requirements for the Degree of
Master of Science

Electrical Engineering

Raleigh, North Carolina

2010

APPROVED BY:

Dr. Srdjan Lukic	Dr. Wenye Wang

Dr. Mesut E. Baran
Chair of Advisory Committee

BIOGRAPHY

Shane Robert Hutchinson was born September 17, 1985 in Springfield, Massachusetts, USA to Robert and Janet Hutchinson. He moved to Colorado in 1998 and stayed there for the remainder of grade school, and then proceeded on to high school in the same area. He received the Bachelor of Science in Engineering with an emphasis on Electrical Engineering from the Colorado School of Mines in Golden, Colorado in 2008. Soon thereafter, he married his wife, Ashley Hutchinson, and moved to North Carolina to pursue a Master of Science degree in Electrical Engineering at the North Carolina State University under the direction of Dr. Mesut Baran.

ACKNOWLEDGMENTS

My deepest gratitude goes toward the people who made this work possible.

To Dr. Mesut Baran, whose advice and extensive knowledge have contributed immensely to the work presented here. Thank you for your guidance and wisdom in the field of power systems.

To Dr. Srdjan Lukic, who constantly gave support and encouragement throughout the course of my studies.

To Urvir Singh, Hossein Hooshyar, Arvind Govindaraj, Zhuoning (Daniel) Liu, Siddharth Ballal, Zeljko Pantic, Ed Van Brunt, Sanzhong Bai, Sumit Dutta, Wei Jing, Zhan Shen, Kaushik Swaminathan, Shashank Bodhankar, Vahraz Farahani, Babak Parkhideh, Habib Eichi, and Arun Kadavelugu. This degree would be achieved in vain if it were done so without your friendships.

To my family for the love and support you have given me my entire life, and for providing me with the opportunity to study and succeed.

And lastly, to my wife, Ashley, without whose cooperation, encouragement, and love I would be lost. Thank you for the countless blessings that you have added to my life.

I am greatly indebted to all of you. Thank you for your support.

TABLE OF CONTENTS

LIST OF TABLES

LIST OF FIGURES

Chapter 1

Introduction

1.1. Background

Increasing consumer interest in clean, domestic, renewable energy has contributed to the rise in Electric Vehicle (EV) and Plug-in Hybrid Electric Vehicle (PHEV) technologies. These vehicles need to be charged with energy from the electric power grid, and while it is well known that they will have the capability to charge from a home garage, availability and use of PHEVs and EVs will lead to the need for charging while away from the home, similar to the refueling of gasoline-powered cars. In contrast with the gasoline-powered car, however, the PHEV and EV can safely charge without being supervised, which allows for more convenient refueling methods such as charging while at work or shopping. This research focuses on the first generation design of a power delivery architecture for a PHEV/EV charging station system to be implemented in a

large parking deck for consumer use. It is expected that the penetration of the PHEV/EV vehicles will be quite rapid during the coming 5-10 years, and such a charging station at parking decks is one of the critical infrastructures which needs to be addressed.

1.2. Thesis Objective

The aim of this thesis is to present the procedure for design and development of a charging infrastructure to be used in a large parking deck in order to charge PHEVs and EVs which are connected to the system. This procedure includes the sizing of cables, transformers, and protective equipment, and a consideration of the effects of harmonics on the transformer.

Each of the procedures used to obtain a final design are outlined in this thesis, and can be replicated for any similar parking deck. The system which is designed here is modular in order to facilitate easy implementation into an existing deck as the EV technology becomes more prevalent.

1.3. Outline

1.3.1. Chapter 2

This chapter covers the basic design of the power delivery architecture, following the National Electrical Code (NEC) [1] and the IEEE Gray Book: Recommended Practice for Electric Power Systems in Commercial Buildings [2]. The procedure for obtaining cable and transformer sizes is outlined, using the Monte Carlo method in order to size for realistic demand as opposed to peak demand. A basic infrastructure is proposed which satisfies all of the constraints, and the design issues surrounding the infrastructure design are addressed.

1.3.2. Chapter 3

Chapter 3 deals with the design of an appropriate electrical protection system for the architecture outlined in Chapter 1. Fuses and circuit breakers are selected in compliance with the NEC. [1]

1.3.3. Chapter 4

The effect of current harmonic contributions from the nonlinear charger loads are characterized and explored in this chapter. The goal is to find what the effect will be on the transformer which is subjected to the harmonic loading.

1.3.4. Chapter 5

Conclusions from the studies are reviewed and future work is presented.

1.4. Glossary of Terms

AC	Alternate current.
Ampacity	The carrying capacity of a cable in amperes corresponding to the loading limit.
Charger	In this study, the word charger refers to the device which converts the power input into the power which is fed to the battery of the PHEV or EV. In AC systems, this device is a rectifier, and in DC systems it is a DC-DC converter.
DC	Direct current.
EV	Electric Vehicle. A vehicle which runs completely on electricity, using only an electric motor to propel the vehicle.
Monte Carlo Simulation	A technique which simulates the output of a complex system by repetitive simulations based on one or more random variables, modeled by probability density functions.

PCC	Point of common coupling. The point at which the utility electric power system is connected to that of the customer, usually at a transformer.
PDF	Probability density function. A statistical distribution that describes the likelihood of an event or distribution of events.
PHEV	Plug-in Hybrid Electric Vehicle. A vehicle with a hybrid mechanical/electrical motor system which has the ability to charge the on-board battery by an external power source.
SOC	State of Charge. The percentage of stored energy remaining in a storage device with respect to the total
THD	Total harmonic distortion. A measure of the amount of harmonics in a certain waveform. The mathematical definition is given in §4.3.1

Chapter 2

Power Delivery Architecture and Component Selection

2.1. Background / Problem Overview

The upcoming generation of PHEVs will have a charger on board which will convert the AC supply to DC, charging the on-board battery. The focus of this paper is the design of an AC distribution supply circuit up to the point of common coupling (PCC) at the plug. Figure 1 shows the main components of the energy delivery from the AC supply to the battery of an EV or PHEV

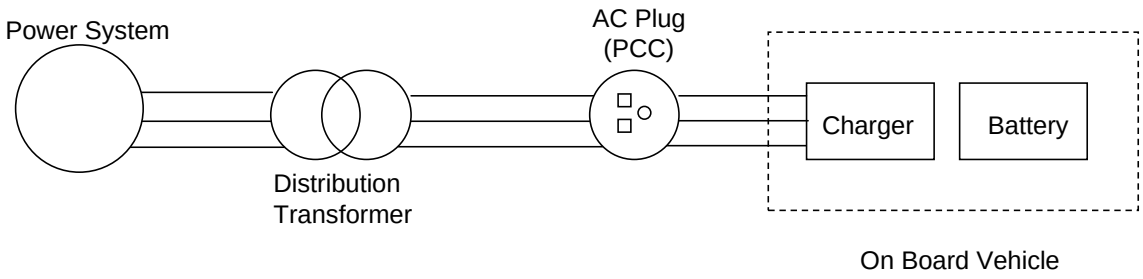

Figure 1: Main Components of System

The SAE J1772 standard [3] defines three charging methods and the ratings of the plugs that will be needed to interface the vehicle's on-board charger with the power delivery system. These specifications will be used to design the delivery system. The standard defines the AC Level 1 charging method using a supply of 120-VAC at a maximum of 12-A continuous current. AC Level 2 charging uses a supply of 240-VAC at a maximum of 32-A continuous current. DC charging is also defined, utilizing an off-board charger which bypasses the lower-rated on-board charger. J1772 uses 600-VDC maximum and 400-A maximum for this level. [3] The first generation charging stations will need a power delivery system for AC Level 1 and AC Level 2 charging. The design of this system is elaborated below.

2.2. Design Challenges

The prototype parking deck considered is a "business parking deck" in an office park with 5 levels and roughly 1700 parking spots. This deck represents a parking structure

common to business lots and has a very predictable pattern of use. The aerial view can be seen in the Appendix, Figure A 1.

One of the challenges faced in using existing parking decks is that the amount of extra space in a parking deck is usually very limited and cannot accommodate a new, large infrastructure on the floor of the deck itself. For this reason, it is desirable that the charging system does not considerably affect the amount of space available for parking. With this constraint taken into consideration, the initial design for the charging system is illustrated in Figure 2. As the figure illustrates, there will be a charging module similar in structure to a parking meter for every two spots in the deck. Each module will need to supply two cars at their maximum demand. As a worst case, the peak power consumption of one charger will be determined by the max current of the AC Level 2 charging. At 32-A and 240-V, as outlined above, this is 7.68-kW.

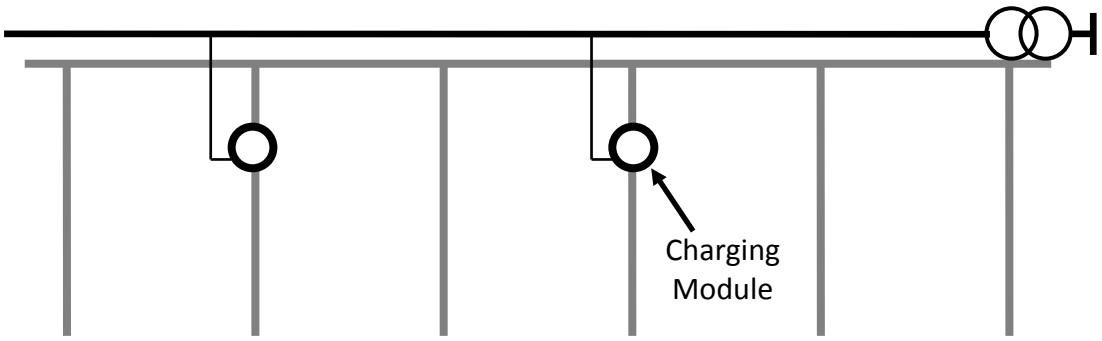

Figure 2: Power Supply Layout for Parking Deck Charging System

Hence, having a large number of charges in such a small space represents a very high density load – a charger operating at 7.68-kW represents the power consumption of

roughly 6 residential houses, based on a US average household consumption of 1.26-kW from the Energy Information Administration [4]. Given that the AC supply is the same as for residential, three wire 240/120-V, such a high density load will require sizeable cables and supply transformers.

Alternate designs were considered for this power supply circuit. We considered wiring the entire deck at a higher voltage, such as 480-V, so that the amount of current could be decreased. However, this became very bulky since it would require transformers at each module, and thus would also be very costly. The other main design which was considered was the use of a central charging station supplied from the transformer, which operated at a higher voltage. This would enable fewer transformers than the previous design, but this was also dismissed because the size of the transformers would be such that they would require a parking space for mounting, and this was an undesirable result.

2.3. Cable Sizing

The proposed design is to wire the parking deck at the standard 240/120-V level, to avoid the need for a transformer at the charging module. In this design, there will be a number of modules strung from one supply cable as shown in Figure 2. Because of the high current rating of each charger, it will only be feasible to supply 1 to 7 modules from the same cable, or 2 to 14 chargers according to standard cable ampacities in the NEC Table 310.16.

In order to size the cable, it is necessary to estimate the total current that will be drawn by the chargers supplied by the cable. The current drawn by a charger during a charging cycle is influenced by the state of charge (SOC) of the battery being charged. A simulation was performed to obtain the current profiles for a typical charger charging a 14-kWh battery and using a constant current, constant voltage DC charging scheme. Figure 3 shows the variation in current profile with different initial SOC of the battery. As the figure shows, there is a diversity observed in the supply current for the various initial SOC values. Since the AC supply voltage is a constant 240-V in the simulation, the power profile follows the same trend.

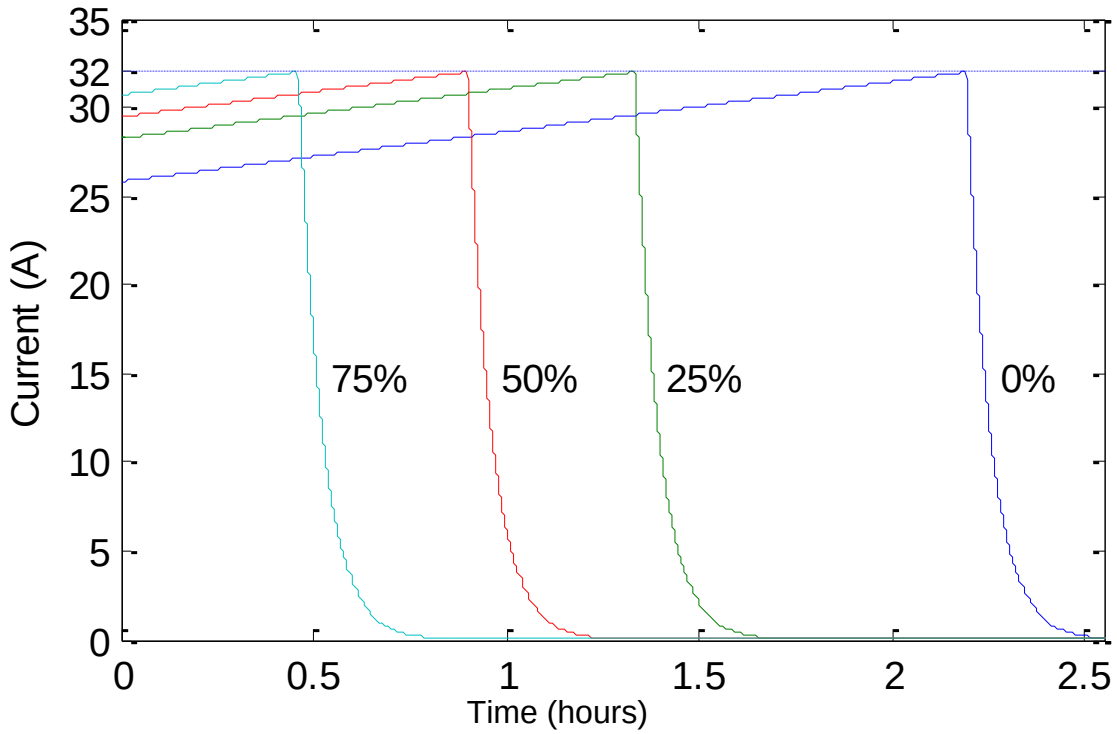

Figure 3: Current Profiles for Various Initial SOC

Diversity in power consumption could have a direct effect on the sizing of cables in this system. If there are 5 chargers being supplied by the same cable, it might be too conservative to use the 32-A as the maximum ampacity of each charger on the line. Hence a Monte Carlo based simulation has been performed to determine the extent to which the variation in initial battery SOC affects the total current level for a given number of chargers.

2.3.1. Monte Carlo Simulation

First, models for the battery and charger were implemented in MATLAB Simulink. The battery model used was an average model from NREL of a Lithium-Ion battery cell [5], scaled up to 14-kWh to model a weighted average of HEV and EV batteries. The battery model can be seen in Figure 4. The assumptions made in the modeling were as follows: ideal converter (100% power transfer) at 0.98PF lagging, DC constant current, constant voltage charging; C/2 charge rate with 32-Arms peak AC Current.

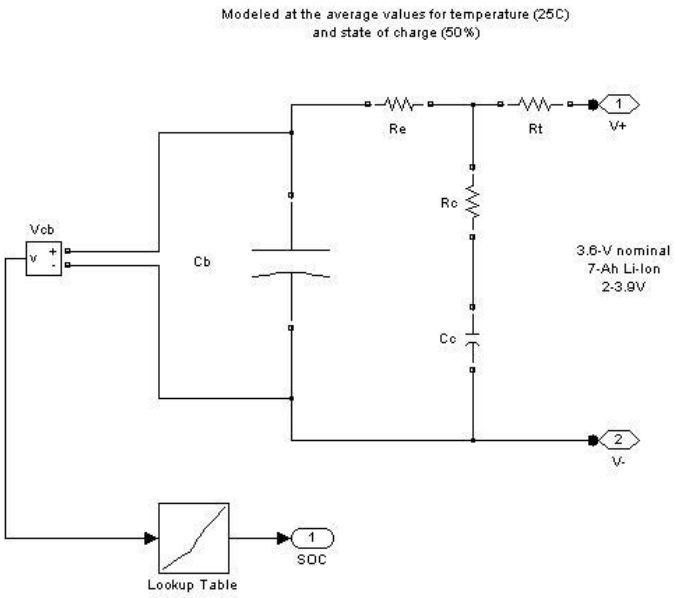

Figure 4: Battery Model

To account for variations in battery SOC, the SOC is modeled as a random variable. The probability density function (PDF) shown in Figure 5 was obtained by using a statistical analysis of the typical distance of a commuter vehicle and the typical battery range on an EV [6]. This PDF is a log-normal distribution with $\mu=3.7$ and $\sigma 2=0.45$.

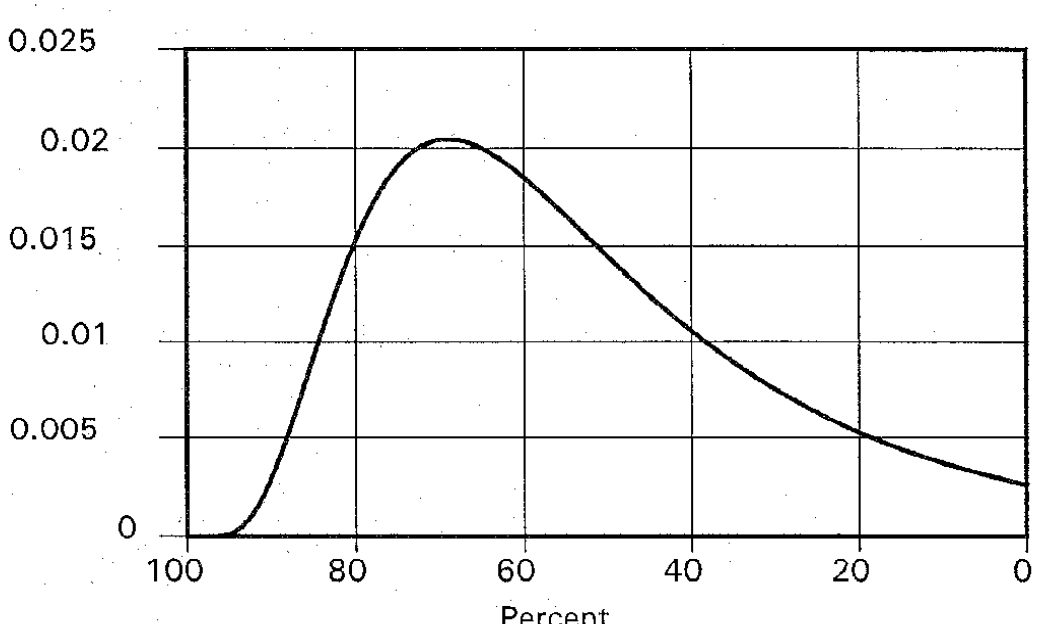

Figure 5: Initial SOC PDF [6]

Using the above PDF to pull a random variable for the initial SOC of the battery, a Monte Carlo Simulation was performed. As a worst case scenario, it was assumed that all charging started at the same time. The simulation was performed for cases of 2 through 14 cars connected to the same cable. With 500 samples per scenario, Figure 6 shows the results obtained.

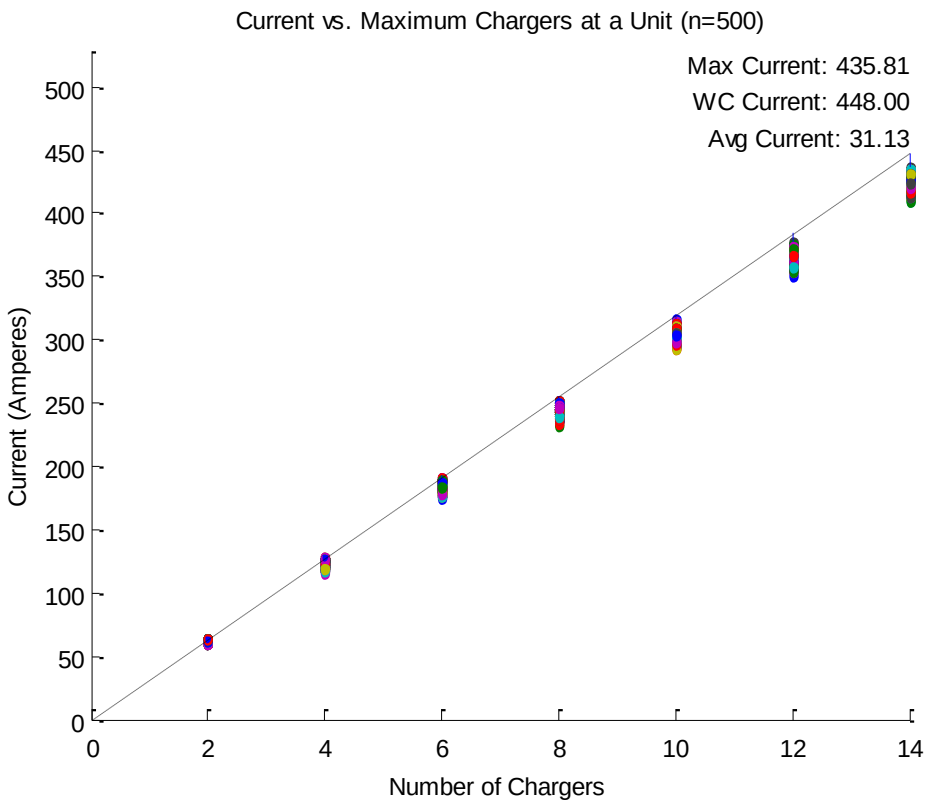

Figure 6: Monte Carlo Simulation Results

The dotted line shows the worst case (WC) current using a simple sum of the max currents connected to the system (i.e. for 6 chargers, WC current is 32A*6 or 192-A). Each dot represents the max current after all simulated charging profiles have been summed. This figure indicates that the maximum current demand from chargers connected to a cable increases linearly even when the initial SOC is taken into account. As seen in the label in the upper-right corner, at 14 chargers the max current of the 500 samples is 438.28-A, which averages to 31.31-A per charger. This figure is not significantly less than the worst case 32-A per charger, and thus it is not justified to use a smaller value for sizing purposes in this scenario. These results show that there is no

advantage in using a larger number of modules connected to a single cable from the diversity perspective.

2.3.2. Results

Based on the simulation results outlined above, a maximum load current of 32-A per car, or 64-A per module was used for sizing the cable, since diversity cannot be taken into account. Thus, the cable will need to have an ampacity in increments of 64-A. The NEC [1] table 310.16 lists the maximum ampacities of various cable sizes and was used to proceed with the cable sizing.

A 2/0 cable was chosen as the best design with the price, voltage drop (maximum length), and installation feasibility taken into account. Figure A 2 in the Appendix shows the results of the comparison in spreadsheet format. It will supply 2 modules (4 spots) with some safety margin, which means that one cable will need to be installed for every 2 AC charging modules. The max length that this cable can be run is about 78-m. A benefit of this design is that it is very modular – the owner of the parking deck can supply multiples of 4 spots instead of installing the infrastructure for many at a time.

2.4. Supply Transformer Design

Given the load density, there must be several supply transformers placed at various locations in a parking deck. Due to the space limitations, these transformers should be small in size. Hence, a Monte Carlo simulation was performed to determine the estimated total load for a transformer supplying a varying number of chargers. If there are many chargers being supplied by the same transformer, it might be too conservative to use the 32-A as the maximum ampacity of each of the chargers in the system.

2.4.1. Monte Carlo Simulation

The number of cars in a section of the parking deck to be charged with power supplied by the transformer is about 50-200. Since all of these cars will not arrive at the same time, the diversity in start times of the chargers needs to be considered in transformer loading.

Data was collected from the prototype parking deck to get the arrival times of cars parking in the deck. The PDF shown in Figure 7 was formed from the collected data between 7:00AM and 10:00AM. The two peaks correspond with 8:00 and 9:00 when employees are arriving for work. This distribution is typical for weekdays in the parking deck.

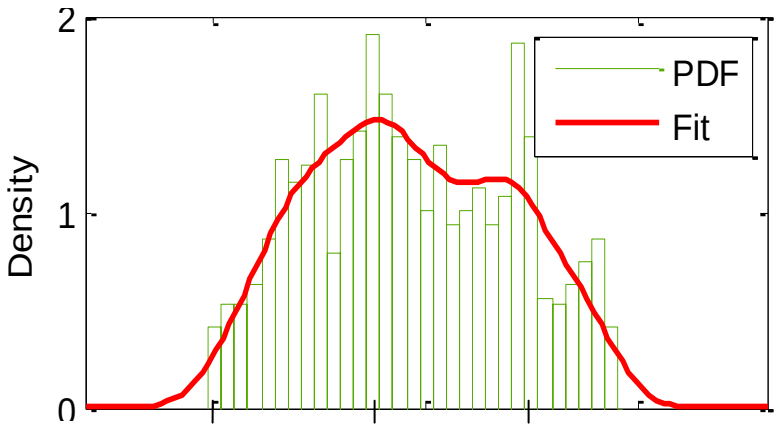

Figure 7: Initial Start Time PDF Fit

Using the PDF obtained for start times and the PDF shown in Figure 5 for the initial SOC of the battery, another Monte Carlo simulation was performed in order estimate the transformer load as a function of the number of chargers supplied. The simulation considered 50 through 200 cars. With 1000 samples per scenario, Figure 8 shows the results obtained.

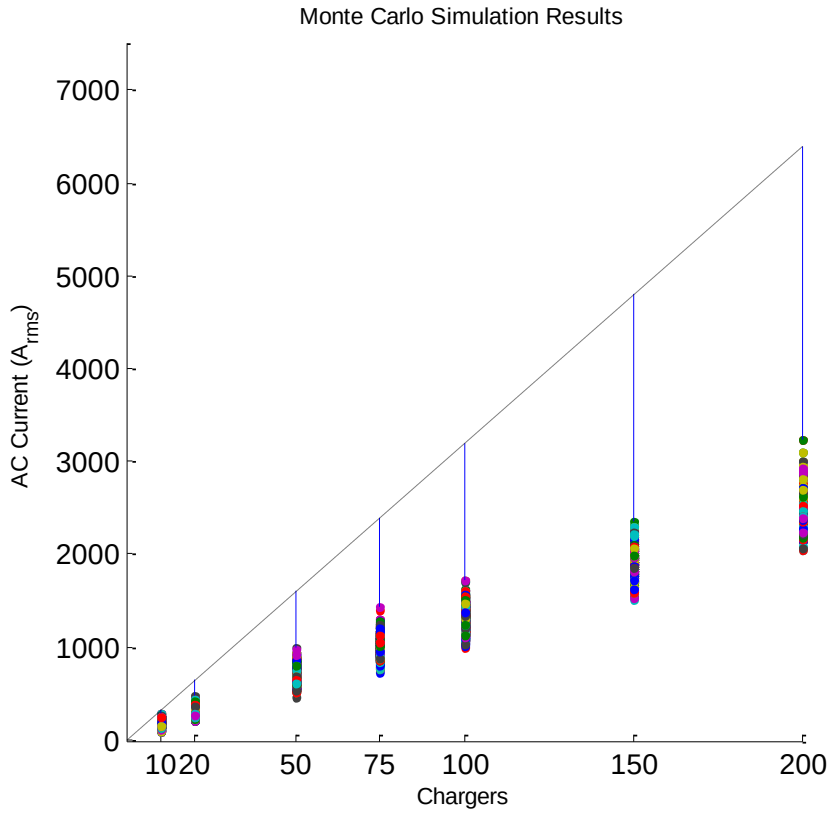

Figure 8: Monte Carlo Simulation Results for Transformer

It is easy to see from the results in Figure 8 that diversity plays an important role when the start times of the chargers are considered along with the state of charge. The small blue line connecting the sampled data to the dotted line shows the effect of diversity by showing the difference between the worst case current and the max of the samples. For example, the max current of the 1000 samples for 200 chargers is about 3-kA, which is 47% of the worst case current. This will be important for sizing the supply transformer.

2.4.2. Transformer Sizing

The Monte Carlo simulation above indicates that, in order to keep transformer size reasonable, a supply transformer is needed to supply a section of a parking deck, since the total load is too high to supply the entire structure with a single transformer. For the prototype deck, the floors are divided into sections of about 40-50 spots, so the transformer will supply 24 modules, requiring 12 cables.

Using the worst case scenario, this design would require a transformer rated at a minimum value of 7.68kW*48 or about 369-kVA. Accounting for diversity and using the results from the Monte Carlo simulation above, this design would require a transformer sized for about 60% of the worst case or about 220-kVA. The 60% figure was obtained by looking at the worst case current for the 50 car simulations in the results shown in Figure 8.

2.5. Summary of Design

This chapter explored the main design issues related to power supply infrastructure needed for a vehicle charging system to be implemented at a large parking deck. The proposed first generation power supply architecture of the charging deck will involve a charging module for every two parking spaces. These modules will provide AC 240/120-V charging plugs for the cars. Every two modules will be supplied by a 2/0 cable at a

distance less than 68-m from the supply transformer. A supply transformer with a rating of 230-kVA is needed for 48 parking spaces.

Chapter 3

Electrical Protection

3.1. Background / Problem Overview

This chapter aims to satisfy the requirement of an electrical protection for the supply circuit in compliance with the NEC [1]. The major design components for the protection system are: the fuse at the primary of the transformer, the main circuit breaker at the secondary of the transformer, the circuit breakers at the panelboard which feed the cables to supply the loads, and the ground fault circuit interrupter at the outlets.

3.2. Method/Procedure

All commercial protection systems must comply with the National Electrical Code [1]. Hence, this code will be used to design the protection of the charging/parking deck. The main sections of the NEC which are used in this design are: 210 (Branch Circuits), 230 (Services), 240 (Overcurrent Protection), and 625 (Electric Vehicle Charging System).

3.3. Design Solution

The one-line diagram for the protection system can be seen in Figure 9 on the next page. This is the culmination of all of the research efforts for the protection system for the charging deck design. The various components are outlined in the following sections.

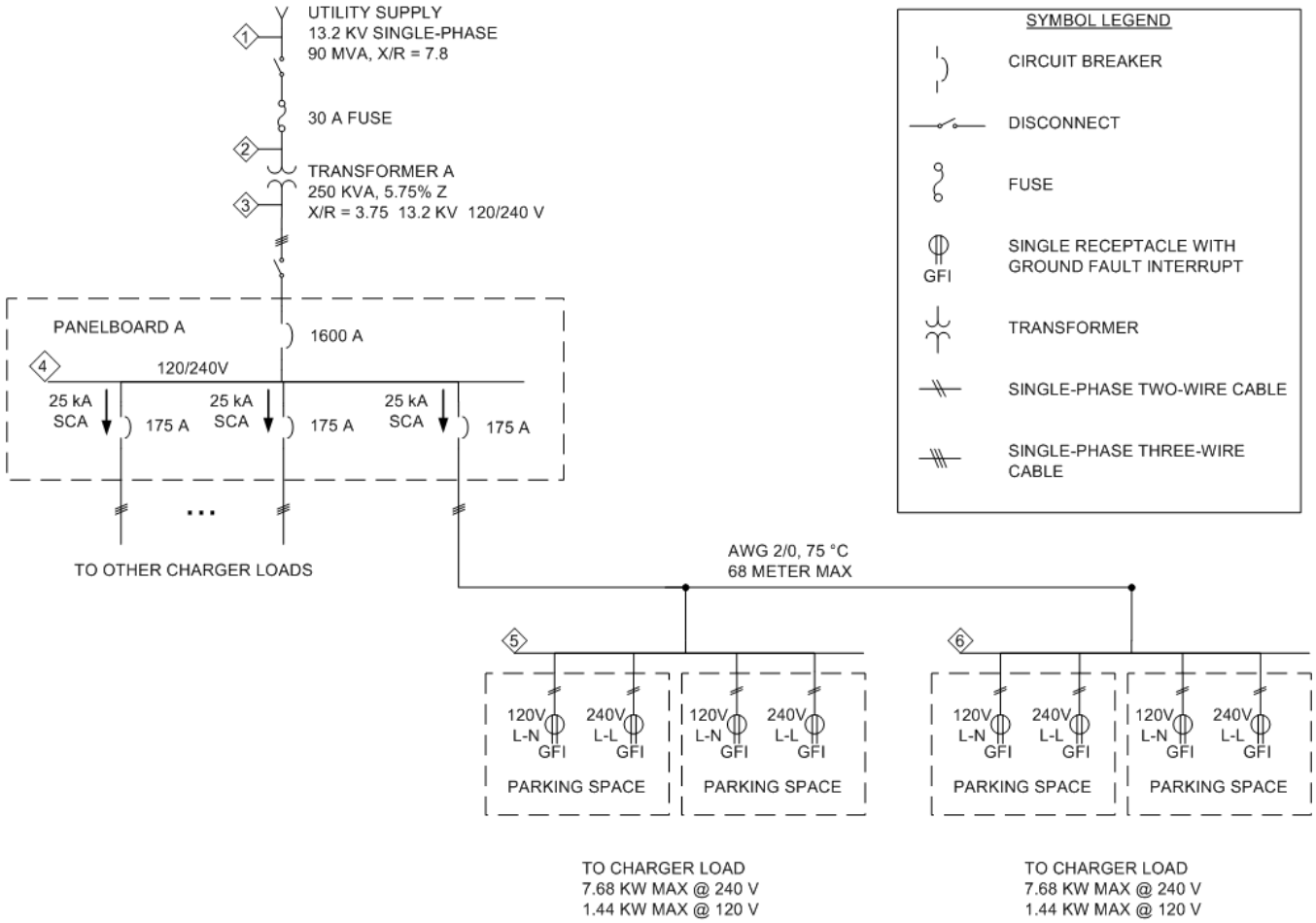

Figure 9: Full System Design

3.3.1. Fuse Selection

According to Cutler-Hammer's sizing guide [7], the fuse on the high side of a transformer should be rated as the rating at or above 1.4 times the full-load current of the transformer. For a 250kVA transformer as outlined in this design, this means that the fuse should be rated for 250kVA/13.2kV*1.4 or 26.5A. The next standard size is 30A [1], so this is the size that should be used.

3.3.2. Panelboard

The panelboard contains two critical protection devices: the main circuit breaker and the feeder circuit breakers. There will be 12 2/0 cables coming from this panel, and thus 12 circuit breakers are required. According to section 230.71 of the NEC [1], since there are more than six protection devices connected to the service, there will need to be a main breaker as well, as shown in the one-line.

3.3.3. Main Circuit Breaker

The main breaker will be rated according to the rating of the transformer. In section 625.21, the NEC states, "Overcurrent protection for feeders and branch circuits supplying electric vehicle supply equipment shall be sized for continuous duty and shall have a rating of not less than 125 percent of the maximum load of the electric vehicle supply equipment." [1] For a 250kVA transformer, the rating of the breaker should be a

minimum of 250kVA / 240V * 1.25 or 1,300A. The next available standard size in §240.6(A) is 1,600A, and this value will be used for the main breaker.

3.3.4. Feeder Circuit Breakers

According to §240.4 of the NEC [1], each of the feeder circuit breakers will need to be rated for at most the ampacity of the cable itself. This means that they should be rated for the 175A ampacity of the cables. Using the same method as in 3.3.3 and a maximum current draw from the supplied chargers of 32A each or 128A total, the rating is determined as 128A*1.25 or 160A. Since 175A is listed as a standard size in §240.6 [1] and fulfills both of these requirements, it will be the rating which is used.

3.3.5. Protection at the Charging Modules

Assuming that the users will be supplying charging cables which comply with the NEC section 623.13 [1], the flexible cords are considered to be protected according to 240.5(3) [1]. This means that there is no required protection for the charging cables. However, §210.8(B) states that all outdoor outlets should have a ground fault interrupt (GFI). Therefore, GFI devices will be included at each outlet.

Chapter 4

Current Harmonic Analysis of PHEV Chargers and Their Effect on Transformer Rating

4.1. Background / Problem Overview

The Generation I design of a plug-and-charge parking deck infrastructure for PHEV and EV charging has been accomplished. The cable sizes, transformer size, and protection scheme for the system have all been selected, and preliminary results have been presented. The next problem to be addressed is the amount of harmonic current caused by the nonlinear charger loads and how it affects the rating of the supply transformer.

4.2. Literature Review

There were multiple papers which were studied for background information on this study. Their methods and results are outlined below.

In [6], the author uses a 480V single-phase charger as the model for all analysis, and thus is limited to this particular charger when drawing any conclusions. This charger was analyzed for harmonic content at various points in the charging profile, and the harmonic current magnitudes and phases were then modeled as random variable based on the distribution that was obtained from the collected data. The THD from the charger at random points in the charge profile was then obtained both by neglecting the phase of the harmonic currents, as well as with the phase values. These results were then compared. The main conclusion from the paper is that in order to have an accurate estimate of the harmonic current injection from a charger, one must take into account the phase shift of the harmonic current. The claim is that there is substantial current cancellation at the super-fundamental frequencies, reportedly up to 50%. In their results, they claim, "The particular densities and charger model chosen for this example indicate a reduction of harmonic currents of approximately 50% from the full-power algebraic solution." [6]

The method used was a statistical one in which the author defined two main functions which give the real and imaginary current components for an input power. From there, the author models the SOC of the vehicle and the start time as a random variable, and finds a final statistical equation to define the expected value and variance at

time t for the real and imaginary components. Their results are then obtained based on these equations.

This paper's shortcomings are that it was conducted on only one charger, making its results less valuable for other charger studies. Another difficulty in applying these results to our study is that it assumes a load other than chargers connected to the grid, which acts to dampen the harmonic influence on the system. In our system, the chargers are the predominant load, with all other loads of negligible size in comparison. However, the procedure that it outlines is very useful, and the Monte Carlo approach will be used in our analysis to do similar analysis.

In [8], the effects of battery chargers on the electric power grid are discussed. Gomez focuses mainly on the harmonic effects, and their impact on the life of the power transformers at the distribution level. A study was conducted to relate various charge times of the day and THD (Total Harmonic Distortion) of the chargers with the life of a transformer.

The focus of this paper was on the effects of the battery charging system on the grid. The areas of harmonics, overloads, and equipment effects were discussed in detail. For his research on harmonics and their impact, Gomez explained that commercial chargers showed THD values as high as 60 or 70 percent.

The authors then go into the analysis of the distortion effects on transformers, cables, and circuit breakers and fuses, which was of value to our studies. The VBA program that was created to analyze the specific effects on transformers showed that in order to have a

"reasonable" increase in transformer life consumption, the THD should be limited to 25 to 30% for each charger. Various graphs and charts were created that showed the effects of the harmonics at different times of the day and for various charge-cycle times.

This study is a bit too basic to be useful in our studies, though the references proved to be useful for IEEE standards. The authors again assume that the majority of the load on the transformer during peak hours is from other devices besides the EV chargers, and thus its results will not prove useful to our studies, where the only substantial load on the transformer is nonlinear charger loads. The basis of their conclusions is strongly dependent on other damping loads on the system.

4.3. Proposed Approach

In order to analyze the effect of current harmonics on the sizing of the transformer, we first needed to characterize the load in concern, taking samples of the charging current at various times during the charge cycle and analyzing the acquired signals for harmonic content. We could then proceed to determine the effects of multiple chargers connected in a system on the supply transformer.

4.3.1. Background

The THD of a signal can be computed as

$$THD = \frac{\sqrt{\sum_{k=2}^{n} I_k^2}}{I_1},$$

where I_k represents the k^{th} harmonic with respect to the fundamental, I_1 and n is the maximum harmonic studied. Note that in the IEEE 519 standard, a value of 50 is used for n [9]. This number will also be used in the studies presented here. While THD is ideal for a comparison of harmonic content between signals, it is not directly used for derating purposes.

The Discrete Fourier Transform (DFT) is used in this study to obtain the current magnitudes at the various harmonic frequencies. The DFT is defined as:

$$X_k = \sum_{n=0}^{N-1} x_n e^{-\frac{2\pi i}{N} kn} \qquad k = 0, \ldots, N-1,$$

where i is the imaginary unit, and N is the length of the discretized signal, and x_n is the sampled signal.

4.3.2. Characterization of Chargers

The first step in our approach was to determine the harmonic characteristics of the chargers in question. Two commercially available hardware battery chargers were tested: the Hymotion PHEV kit for the Prius HEV, and the Progress Energy Ford Escape PHEV. Along with those two, a third charger was considered: the proposed NCSU ATEC charger which is simulated.

A charge cycle for each of the chargers was observed and the current waveforms were sampled by use of a Tektronix scope in the case of the commercial chargers, and sampled from the simulation in the case of the ATEC charger. For the hardware chargers, the supplied charging cord was connected to the 120V power supply at the lab. A current transformer was connected to measure the current flowing to the charger, and a voltage transformer was connected to measure the voltage of the line, as shown in Figure 10. The specs for the measurement equipment are attached in the Appendix.

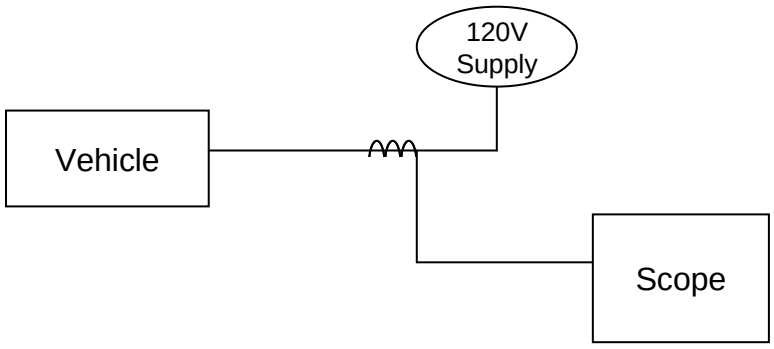

Figure 10: Measurement Setup

4.3.2.1. Prius Charger

We cannot be sure of the initial state of charge of the Prius at the time of data collection. However, the charge started and finished in about 2 hours, which gives an idea about the length of charge that was examined. Based on that, it is estimated that the initial state of charge was around 50%. The data was sampled at 8μs intervals for 2.5 cycles of the signal. The waveform was triggered at the zero crossing of the voltage waveform to ensure that any comparison among signals took the power factor into account. There are a total of 111 samples spanning the charge cycle. 5 samples were taken roughly every 5 minutes for the duration of the charge, and their corresponding waveform raw data were saved to a .dat file. A sample waveform is shown below.

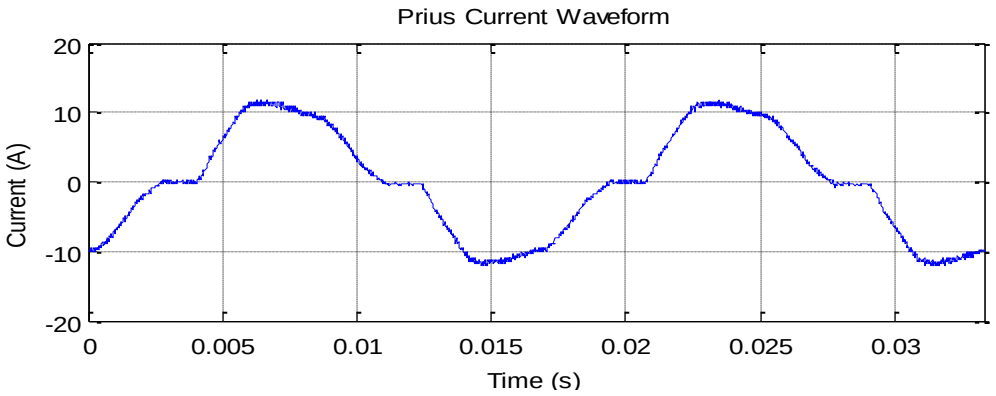

Figure 11: Sample Prius Current Waveform

From this waveform, it is speculated that the Prius charger uses a rudimentary diode-bridge rectifier with minimal power factor correction. Using a DFT of the above signal, the harmonic currents from the 1st through the 50th were computed. They are shown in Figure 12.

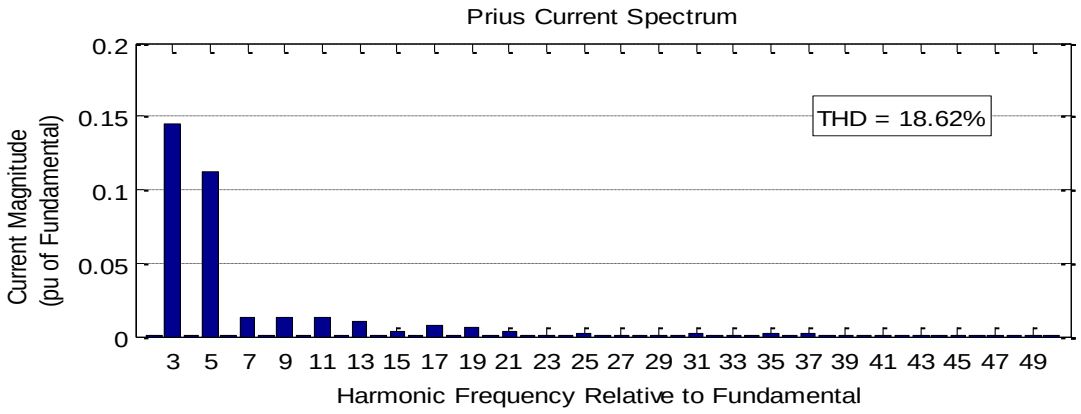

Figure 12: Prius Current Spectrum

The mean THD from the Prius was 17.31% with a standard deviation of 1.29% for the 111 samples. This value is very high for use in a commercial charging system with no other loads to dampen the harmonic effects. The bar graph below shows the mean harmonic content (the bars), as well as the standard deviation in the error bars. The THD values given and in the upper right corner of the figure were computed with harmonic currents up to the 50^{th}, but for simplicity, only the 2^{nd} through the 15^{th} are shown in the bar graph. The harmonics above the 15^{th} are very small and not necessary to show here.

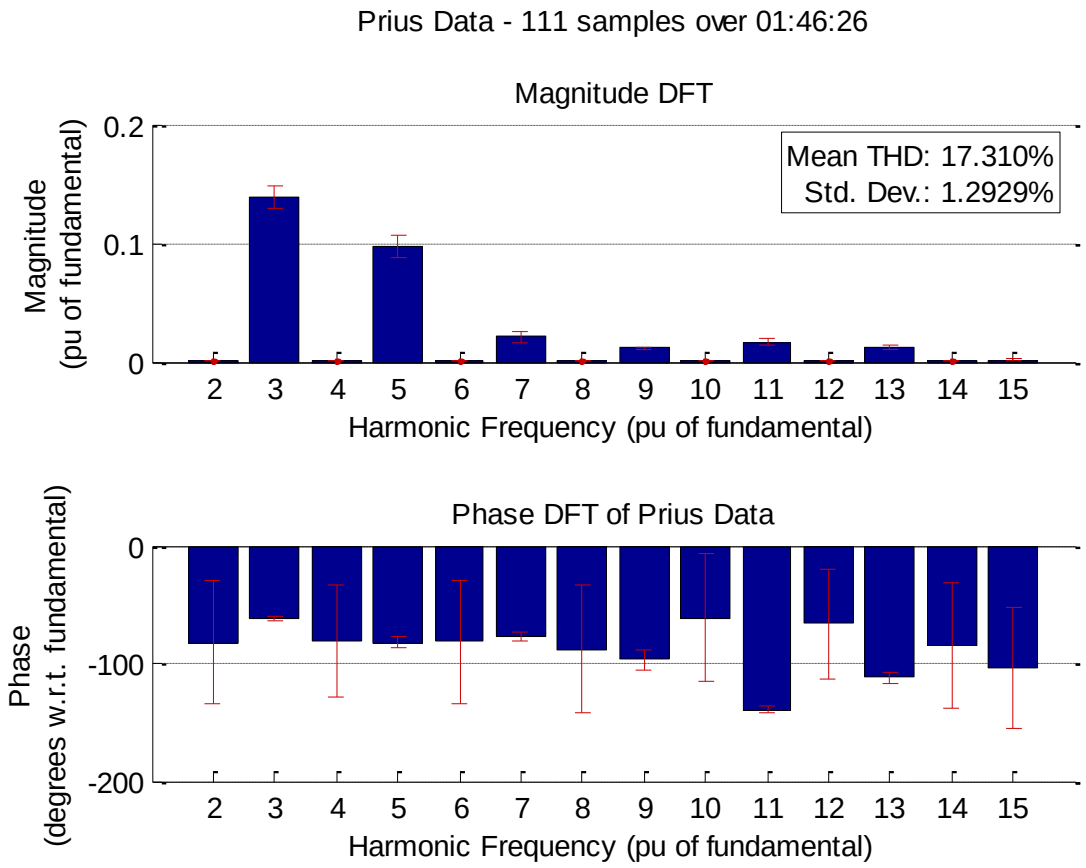

Figure 13: Prius Harmonic Summary

Note that the standard deviation of the magnitudes and phases are relatively small throughout the duration of the charge cycle. The largest deviations are for the even harmonics' phases, and that is expected for the corresponding small magnitudes.

4.3.2.2. Escape Charger

The reading on the on-board SOC estimator for the Escape was 44% when we began the charging cycle. This was reported to be about as low as it will go due to battery life precautions. The data was sampled for a duration of about 6 hours at 3 samples every 5

minutes. Each sample was taken at 4μs intervals, which is double that of the Prius data. Also, each dataset sampled represents about 6 waveforms at the fundamental 60Hz. There are a total of 253 samples spanning the charge cycle. As in the case of the Prius, the waveform raw data was triggered at the zero-crossing of the voltage signal to account for power factor, and was written to a .dat file on the hard disk. A sample waveform of the Escape is shown below.

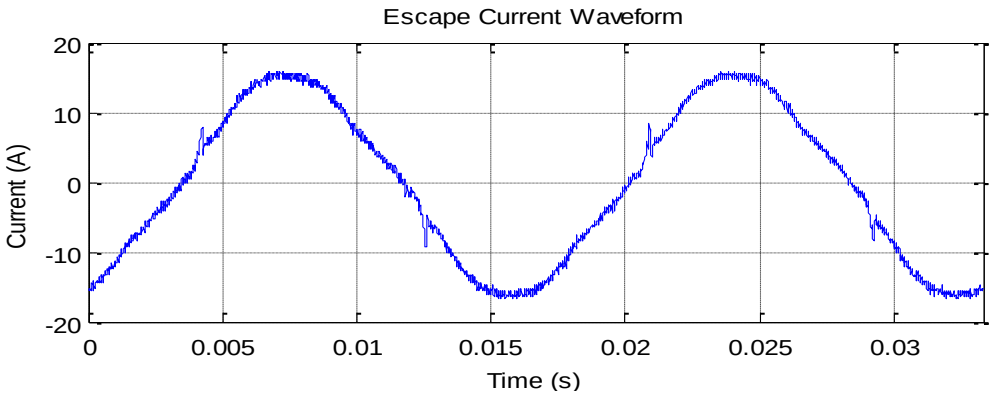

Figure 14: Sample Escape Current Waveform

This waveform reveals that the Escape charger uses much more power factor correction than the Prius, although it is unclear what the exact topology is. The harmonic currents are shown below.

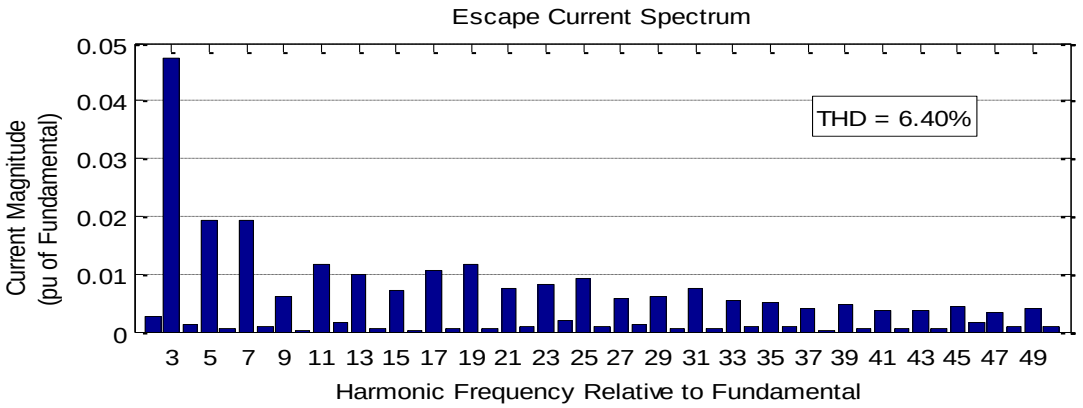

Figure 15: Escape Current Spectrum

The mean THD from the Escape was 6.48% with a standard deviation of 0.135% for the 253 samples. This amount is more reasonable than that of the Prius. The mean and standard deviations for each of the harmonic currents through the 15th can be seen below.

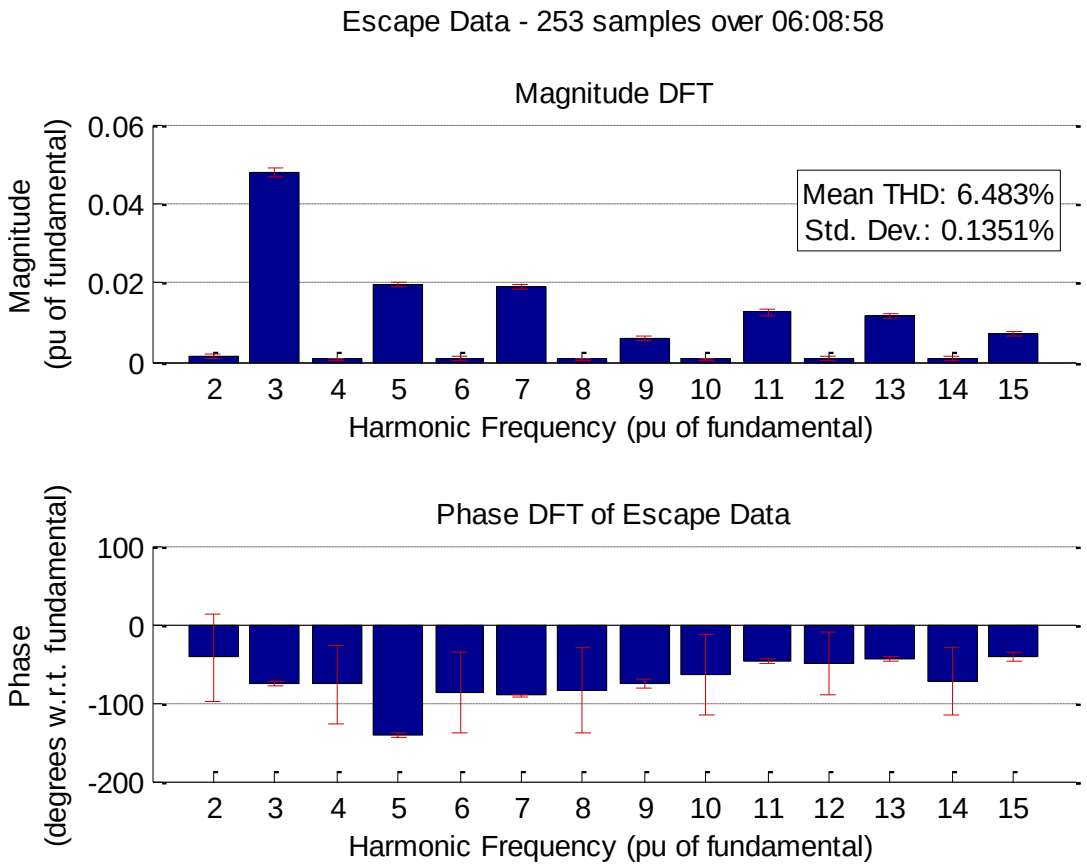

Figure 16: Escape Harmonic Summary

4.3.2.3. ATEC Charger

A switching-model simulation was provided by Xiaohu Zhou for ATEC's Generation II charger. The model is a 2-stage converter with an AC PWM rectifier stage and a DC stage. The DC current reference was set to give a maximum of $32A_{rms}$, and the battery was charged at constant DC current. The simulation was run for 5 cycles at varying SOC values from 0% by 2% to 90%. The current waveforms were then saved to the disk to be analyzed in the same way as the Prius and Escape data.

The battery model which was used in this simulation is the same battery model that was used for the simulations in Chapter 1 [5], and was scaled to represent a 10kW, 288V battery unit. A sample waveform from the ATEC charger is shown below.

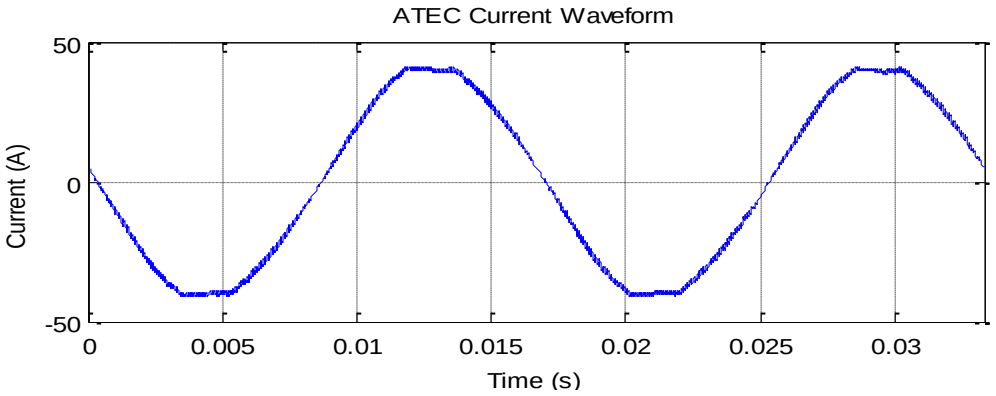

Figure 17: Sample ATEC Current Waveform

Using the same DFT analysis as in the previous two cases, the above waveform gave the following spectrum.

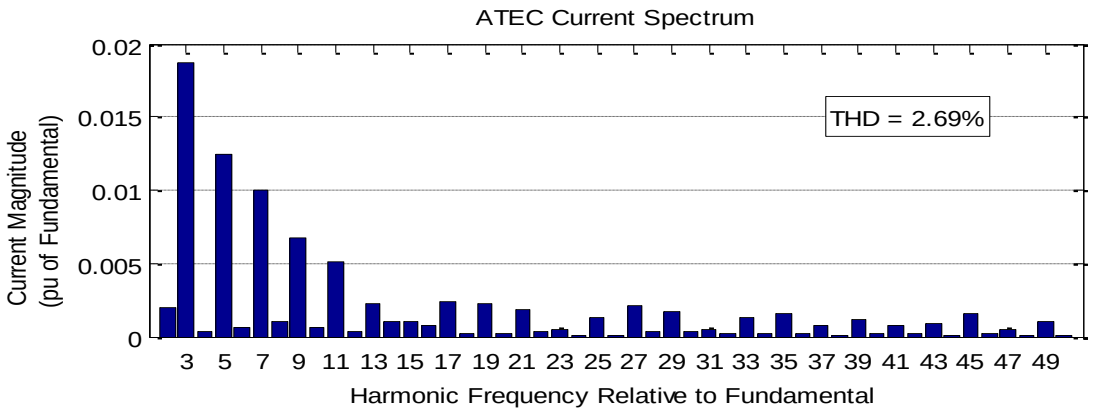

Figure 18: ATEC Current Spectrum

The mean THD from the ATEC charger was 2.626% with a standard deviation of 0.0869% for the 46 samples. This is a significantly smaller value than the Prius, and also

improved from the Escape. The mean and standard deviations for each of the harmonic currents through the 15th can be seen below.

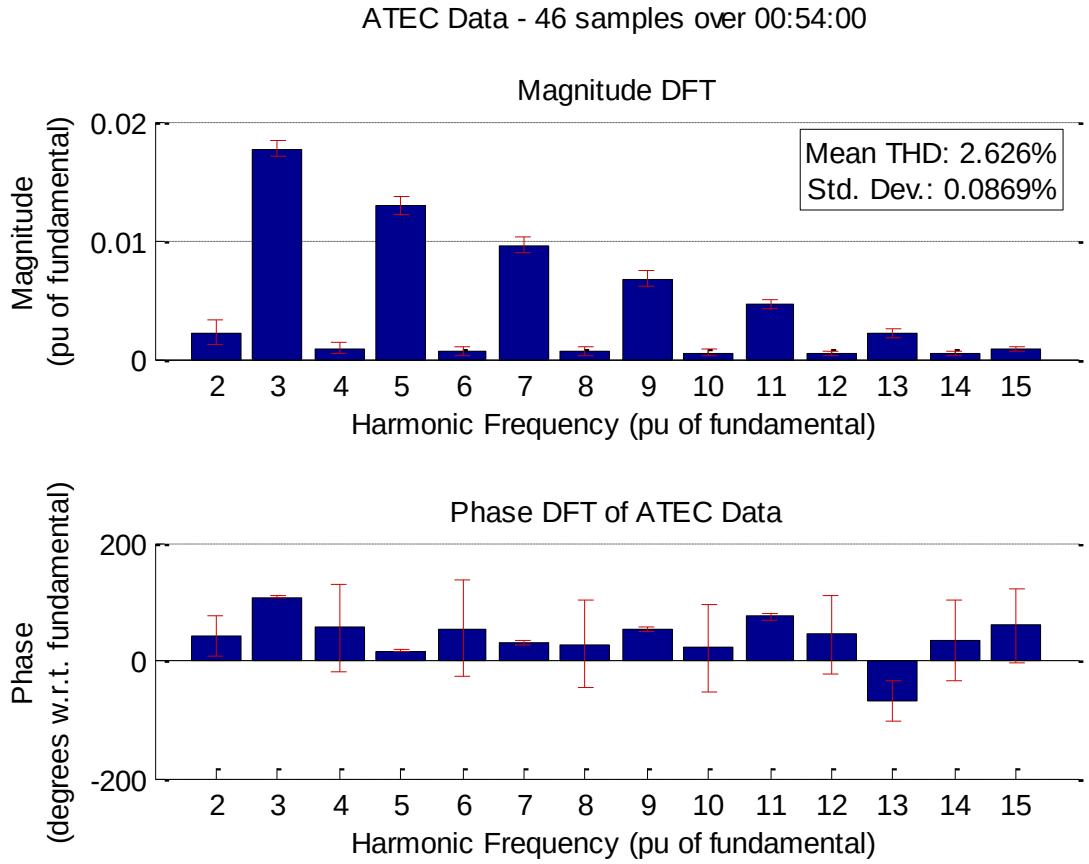

Figure 19: ATEC Harmonics Summary

4.3.2.4. THD Comparison

The following figure shows a comparison of the expected values and standard deviations of the THD content for each of the three chargers.

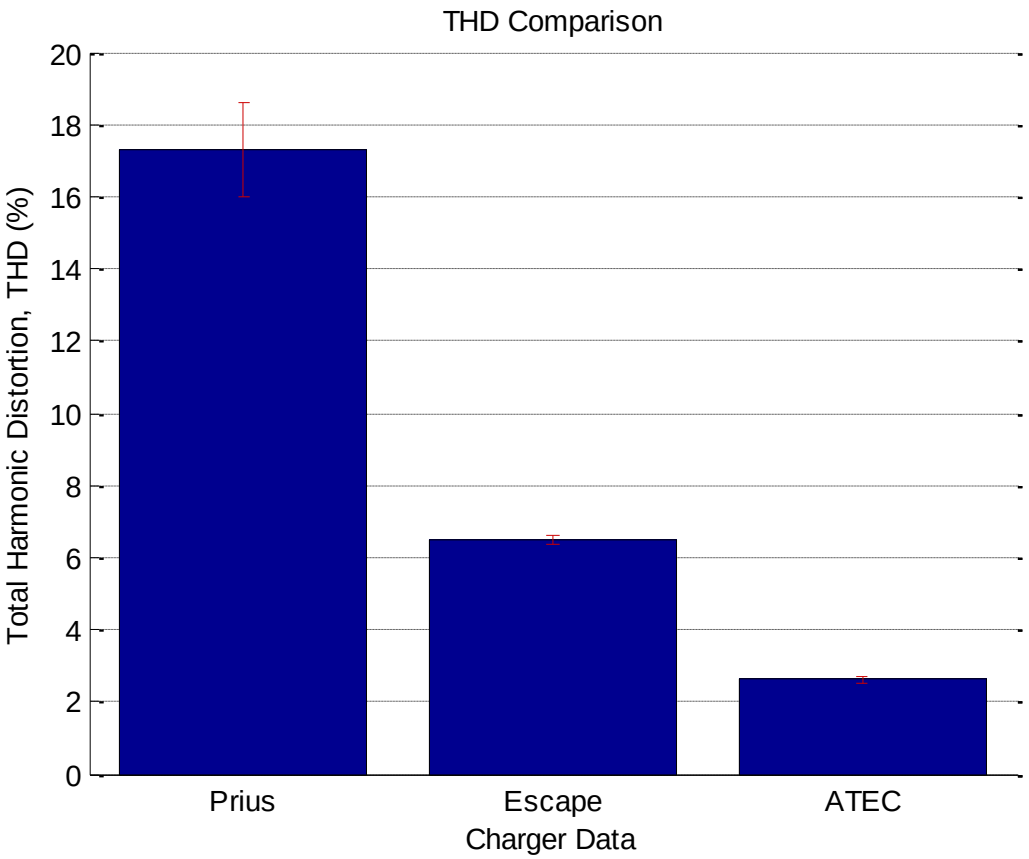

Figure 20: THD Comparison

As can be seen, the Prius has a substantially higher THD value than the others. All three show little variation in the THD content, according to the standard deviation shown in the error bars.

4.4. Data Analysis

Now that the chargers have been characterized, the necessary analysis can be performed. In this study, we are interested in the effect of the harmonic current on the sizing of the distribution transformer. The procedure used for transformer derating from non-sinusoidal currents was the IEEE C57.110 [10]. As mentioned previously, the frequencies considered in this study were from the 1^{st} harmonic to the 50^{th} in accordance with IEEE 519 [9].

4.4.1. IEEE C57.110 Transformer Derating Calculation

The IEEE C57.110 [10] specifies the method for determining the derating factor for a transformer which is under heavy non-sinusoidal loading conditions. The following tables show the calculations outlined in this standard. The cells with a light background color represent the inputs. The desired output for derating purposes is the I_{max} variable; it specifies the maximum RMS current in per unit that the transformer can withstand at constant loading for a load with a specified harmonic spectrum. This spectrum is input in column B in Table 1 with respect to the fundamental current, along with a value for P_{EC-R}. A conservative value of 0.15 was assumed for P_{EC-R} per the example shown in the standard [10]. The equations which are used in this table are:

$$I_{\max}(\text{pu}) = \sqrt{\frac{P_{\text{LL-R}}(\text{pu})}{1+F_{\text{HL}}\times P_{\text{EC-R}}(\text{pu})}} \quad \text{pu} \tag{1}$$

$$P_{\text{LL-R}}(\text{pu}) = 1 + P_{\text{EC-R}}(\text{pu}) + P_{\text{OSL-R}}(\text{pu}) \quad \text{pu} \tag{2}$$

$$F_{\text{HL}} = \frac{\sum_{h=1}^{h=h_{\max}} \left[\frac{I_h}{I_1}\right]^2 h^2}{\sum_{h=1}^{h=h_{\max}} \left[\frac{I_h}{I_1}\right]^2} \tag{3}$$

$$P_{\text{LL}}(\text{pu}) = I(\text{pu})^2 \times (1 + F_{\text{HL}} \times P_{\text{EC-R}}(\text{pu})) \quad \text{pu} \tag{4}$$

Where the variables are defined as follows:

h	is the harmonic order
Ih	is the rms current at harmonic "h" (amperes)
F_{HL}	is the harmonic loss factor for winding eddy currents
P_{EC-R}	is the per-unit winding eddy-current loss under rated conditions
P_{OSL-R}	is the per-unit other stray loss under rated conditions (neglected here)
I_{rms}	is the total rms current as calculated from C12 in the table
P_{LL}	is the per-unit load loss
P_{LL-R}	is the per-unit load loss under rated conditions
I_{max}	is the max permissible rms nonsinusoidal load current under rated conditions

Table 1: Calculations for derating factor per C57.110

	A	B	C	D	E	F	G	H
1	**h**	**I_h/I_1**	**$(I_h/I_1)^2$**	**h^2**	**$(I_h/I_1)^2h^2$**		**F_{HL}**	**=E12/C12**
2	1	###	=B2^2	=A2^2	=C2*D2		**P_{EC-R} (pu)**	###
3	3	###	=B3^2	=A3^2	=C3*D3		**I_{rms} (pu)**	=SQRT(C12)
4	5	###	=B4^2	=A4^2	=C4*D4		**P_{LL} (pu)**	**=H3^2*(1+H1*H2)**
5	7	###	=B5^2	=A5^2	=C5*D5		**P_{LL-R} (pu)**	=H2+1
6	9	###	=B6^2	=A6^2	=C6*D6		**I_{max} (pu)**	**=SQRT (H5/(1+H1*H2))**
7	11	###	=B7^2	=A7^2	=C7*D7			
8	13	###	=B8^2	=A8^2	=C8*D8			
9	15	###	=B9^2	=A9^2	=C9*D9			
10	17	###	=B10^2	=A10^2	=C10*D10			
11	19	###	=B11^2	=A11^2	=C11*D11			
…	…	…	…	…	…			
N	Σ		=SUM(C2:C(N-1))		=SUM(E2:E(N-1))			

An example of this calculation for a Prius sample data can be seen in the following table.

Table 2: Example calculation for derating factor

h	I_h/I_1	$(I_h/I_1)^2$	h^2	$(I_h/I_1)^2h^2$		F_{HL}	**1.4546**
1	1.0000	1.0000	1	1.0000		P_{EC-R} **(pu)**	0.1500
3	0.1239	0.0153	9	0.1381		I_{rms} **(pu)**	1.0120
5	0.0857	0.0074	25	0.1838		P_{LL} **(pu)**	**1.2477**
7	0.0239	0.0006	49	0.0280		P_{LL-R} **(pu)**	1.1500
9	0.0144	0.0002	81	0.0168		I_{max} **(pu)**	**0.9716**
11	0.0202	0.0004	121	0.0494			
13	0.0159	0.0003	169	0.0429			
15	0.0023	0.0000	225	0.0011			
17	0.0078	0.0001	289	0.0177			
19	0.0058	0.0000	361	0.0120			
Σ		1.0242		1.4899			

The results show that the transformer can carry up to 0.9716 per unit of its rated current if it is subjected to a load with the harmonic profile shown in the second column. This number may be used as the derating factor on the capacity of the transformer.

4.4.2. Derating Factor for Each Charger

The following graphs show the derating factor, I_{max} for each of the chargers at the various data points throughout each of their charge cycles. That is to say, if the sample

collected at each point were applied to the IEEE C57.110 procedure, the graphs show how the parameter would vary for each charger.

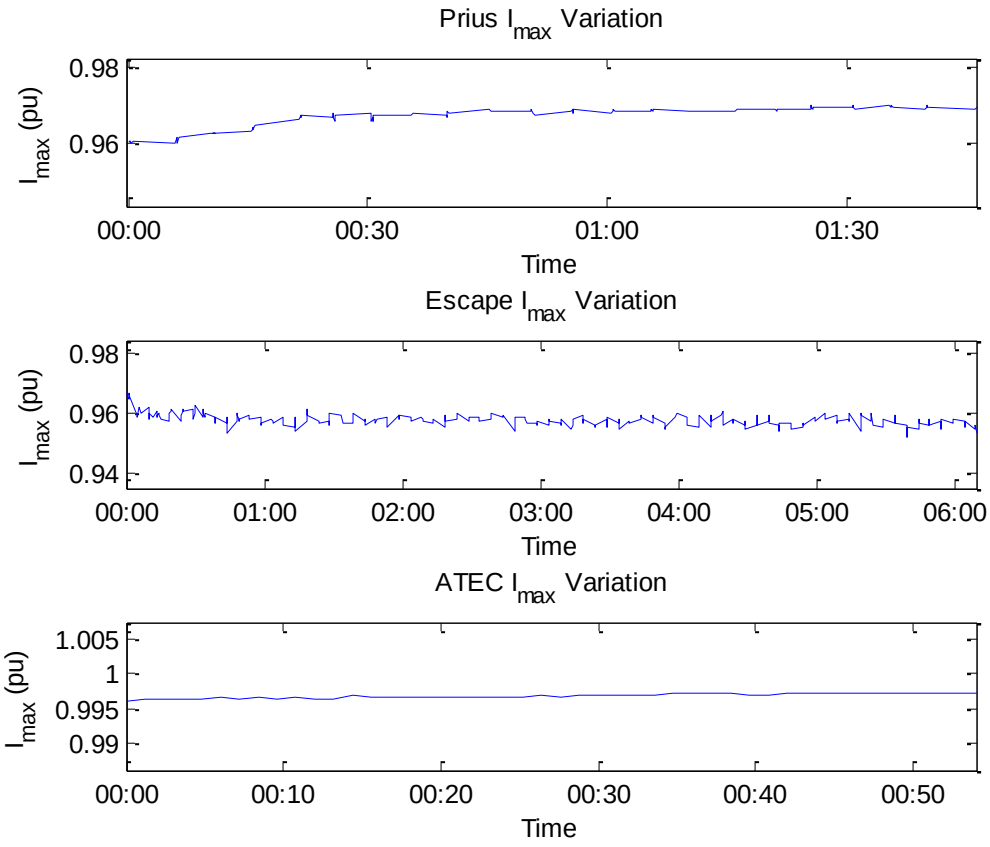

Figure 21: I_{max} Variation

The statistical analysis of the above results can be seen below.

Table 3: I_{max} Comparison

Charger	Mean I_{max} (pu)	Std. Dev. I_{max} (pu)
Prius	0.9670	0.0028
Escape	0.9581	0.0022
ATEC	0.9968	0.0003

This table shows that, surprisingly, the Escape gives the worst I_{max}. This was unexpected, since the THD was highest for the Prius charger, but can be attributed to the high order harmonics in the Escape waveform. Equation 3 shows that I_{max} varies with the square of the harmonic order. This was verified by reducing the number of harmonics used in the calculation. In that case, the Escape showed a larger value for I_{max} than the Prius (0.9769 versus 0.9683 for 30 harmonic frequencies). This shows that the THD value can be misleading when determining the effect on the supply transformer.

The table also shows that the variation of the calculated I_{max} is also relatively small. The standard deviation is largest in the Prius values, where it is about 0.3% of the mean value.

4.4.3. Diversity Effects on Derating factor

4.4.3.1. Problem

The parking deck is made up of sections of 48 cars per transformer. The diversity of the harmonic currents injected by multiple chargers may have an effect of reducing the distortion at certain harmonics due to a phenomenon known as harmonic cancellation, as shown in [6]. Thus, the next step was to combine charger data sets together in order to analyze the impact of diversity on current harmonic levels. The hypothesis was that the varying topologies and controls would produce harmonics of different phases, which would have a cancellation effect, lowering the expected harmonic distortion from the strict arithmetic sum of the magnitudes that could be achieved by taking an average of all the THD percentages present in the system.

4.4.3.2. Procedure

The Prius and Escape data sets were used, since they showed the highest harmonic distortion and would thus provide the optimal chance for harmonic cancellation. If significant cancellation is found, the same method can be applied to include the ATEC charger. If, however, the cancellation is not significant, there will be no need to further study this phenomenon and a worst-case arithmetic sum of the harmonic levels can be used in the derating calculation.

Various situations were analyzed using a Monte Carlo simulation approach in a MATLAB program. For a given Prius penetration, the program would randomly pull the corresponding number of charger data points from the data pool for both charger types. For example, 0.25 Prius penetration would yield 12 Prius chargers and 36 Escape chargers, pulled from the pool with a flat random distribution. This distribution is justified since the harmonic levels and phases do not vary considerable amounts throughout the charge cycle, as demonstrated in Figures Figure 13, Figure 16, and Figure 19. The even harmonic phases show quite a variation, but their corresponding magnitudes are small, so the amount of cancellation will be minimal.

The program would then compute the I_{max} value of the configuration using only a strict arithmetic sum of the magnitudes and the I_{max} value of the configuration when the phases of the harmonic currents have been taken into account. 1000 such iterations are performed on each penetration value for reproducibility.

4.4.3.3. Results

The following table outlines the results of this simulation.

Table 4: Monte Carlo Results for 48 chargers, 1000 Samples per Simulated Configuration

Prius Penetration (pu)	**Mean I_{max} w/out Phase (pu)**	Std. Dev. I_{max} w/out Phase (pu)	**Mean I_{max} w/ Phase (pu)**	Std. Dev. I_{max} w/ Phase (pu)	**Mean Increase (%)**	**Std. Dev. Increase (%)**
0.00	**0.9586**	0.00032	**0.9596**	0.00033	**0.1049**	0.0065
0.25	**0.9652**	0.00049	**0.9726**	0.00061	**0.7649**	0.0217
0.50	**0.9697**	0.00043	**0.9805**	0.00036	**1.1061**	0.0232
0.75	**0.9709**	0.00035	**0.9801**	0.00025	**0.9491**	0.0432
1.00	**0.9672**	0.00046	**0.9681**	0.00024	**0.0966**	0.0362

Column 1 gives the per unit penetration of the Prius chargers connected to the system. This means that the Escape penetration would be 1 minus this value. Notice that the first and last rows give the comparison for a system with only Escape models and only Prius models, respectively. The second column gives the mean I_{max} of the combined system by the strict arithmetic sum of the magnitudes of the harmonic currents, neglecting any phase cancellation. The third column is the corresponding standard deviation for column two. The fourth column gives the mean I_{max} with the phases of the corresponding harmonic frequencies taken into account, and the fifth gives its

corresponding standard deviation. The sixth and seventh columns give the mean and standard deviation of the percentage increase in I_{max} (thus the decrease in the amount of derating) between the two cases.

4.4.3.4. Conclusions of Harmonic Cancellation Study

The harmonic cancellation effect yields very little change on the derating factor for the transformer. The largest increase in the I_{max} parameter was when half of the chargers were Prius and half were Escape, yielding a 1.1% increase, which is insufficient evidence to require further investigation. Thus, the simple arithmetic sum of the magnitudes of the currents at corresponding harmonic frequencies can be used to obtain the value of I_{max} and will not provide a significant overestimation.

4.4.4. Applied Derating Factor

With the above results, it can be seen that (1) the I_{max} value does not vary greatly for each individual charger type and (2) there is not significant phase cancellation among the charger topologies. Using these results, it was determined that the worst case I_{max} value can be used to size the transformer without significant over sizing. This value was seen in the Escape at **0.95 pu**. This will be the derating factor used for the transformer.

For the design in the transformer for the case considered in the previous chapter, this would suggest that, although the transformer is rated at 250 kVA, it would only be able to carry 0.95*250 kVA or 237 kVA. In this case, the transformer is still able to supply the maximum load, which was determined to be 230 kVA.

4.5. Summary

A harmonic current analysis was carried out for the charging cycles of the Hymotion Prius PHEV, the Ford Escape PHEV, and the simulated Generation II ATEC charger. Their current profiles during charging mode were analyzed. Data was collected from an oscilloscope, and the waveforms were analyzed for harmonic content. The mean THD for the Prius with Hymotion pack was 17.27% with a standard deviation of 1.30%, while the mean THD for the Escape and the ATEC charger were significantly lower at 5.85% and 2.56% with standard deviations of 0.12% and 0.08%, respectively.

The procedure for determining a transformer derating factor, I_{max} was outlined and carried out for the charger data. It was found that harmonic cancellation does not play a significant role in changing the value of this parameter, and thus can be neglected.

It was shown that the THD and I_{max} values are not strictly related since the I_{max} calculation uses the square of the harmonic order as a multiplier. This showed that the THD value can be misleading when deciding the effect that a certain harmonic current can have on a transformer; while the Escape had a significantly lower THD than the Prius, the amount of derating needed was actually higher, on average.

Because I_{max} does not vary greatly, it is a conservative but not inaccurate conclusion to use the worst case I_{max} value between the three charger types. This value was 0.95 per unit, which signifies that the transformer carrying the harmonic load can only carry 95% of its rated current.

Chapter 5

Conclusion and Future Work

5.1. Conclusions

In this study, a design methodology for a power supply system for supplying a large set of PHEV chargers in a parking deck has been developed. This supply circuit was designed for Level I and Level II charging in accordance with the IEEE SAEJ1772 standard for PHEV and EV plugs. [3] The specific parking deck which the system was designed for is a business deck with a predictable usage pattern.

Between every two parking spaces will be a charging module housing both 120V and 240V receptacles for both adjacent parking spots. There will be two of these modules fed from a single supply cable coming from the distribution transformer. The concept of diversity was looked into for the sizing of these cables with the initial SOC of the connected vehicles modeled as a random variable based on the study in [6], and it was

concluded that 4 spots did not supply sufficient variability in the load current based on Monte Carlo simulations. Thus, the cable was designed for the peak amperage, 128A. The selected cable size of 175A ampacity leaves enough margin for a circuit breaker and the specified 125% safety margin as specified in the NEC. [1]

It was decided based on the arrangement of the prototype deck that the transformer should supply 48 chargers max, meaning 12 cables or 24 modules. Again, diversity was looked into for the design capacity. This time, the arrival times of the vehicles were also modeled as random variables based on the recorded arrival times from the deck in question along with the initial SOC. Diversity in this case showed to have a large effect on the sizing of the transformer, and the results showed that the transformer could be sized for 60% of the peak load based on this study. With this taken into account, the transformer size was determined to be 250kVA.

Protection was then considered for the power architecture. The sizing of the circuit breakers in accordance with the NEC was 175A. These breakers will be placed at the panel for each cable as described above. Since there are 12 cables each with breakers, the NEC specifies that a main breaker needs to be installed. Thus, a main breaker was sized to be 1600A and put up-stream of the others. The transformer will have a fuse on the high side for protection, sized at 30A. Additionally, there will be GFIs at the receptacles for additional protection in case of rain or misuse.

To conclude the studies, a harmonic current analysis was carried out for the Toyota Prius with Hymotion aftermarket PHEV kit, the Ford Escape, and the ATEC charger.

During the charge cycles of each, the 1st through the 50th harmonics were observed, and results were documented. The Prius had a mean THD of about 17% with a standard deviation of 1.3%, the Escape had a mean THD of 6.48% with a standard deviation of 0.14%, and the ATEC charger had a mean THD of 2.6% with a standard deviation of 0.09%.

With the collected data, a derating factor was computed for various scenarios of charger mixing in the deck based on the IEEE C57.110 standard [10]. Diversity was looked into with the harmonic phase cancellation taken into account for random initial states of charge, and it was concluded that there was not significant cancellation in any scenario. As a result, the final value to be used for the transformer derating was determined to be 0.95 per unit. For this value, the 250kVA transformer which was sized in the previous results is sufficient to carry the harmonic load.

With the given results, a charging infrastructure can be implemented in the prototype parking deck, which will be able to supply power to 48 PHEV/EV parking spots.

5.2. Future Work

From this research, it has become apparent that more facets of this topic need to be covered. Specifically, it would be beneficial to get a better representation of the SOC probability distribution for PHEVs and not just EVs. There are additional factors which could change the pdf presented in the referenced paper such as how hard the cars are driven and thus how often the IC engine is turned on, etc.

Another item that should be looked at in more detail is the variability of the harmonics in the measurements presented in this work. Specifically, it is noted that the ATEC charger showed the same large standard deviation of phase values for the even harmonics as did the hardware measurements, showing that it is not due to measurement error alone. Looking into the causes of this phase variation would be very helpful to future studies of this kind.

Lastly, it should be assessed how accurate the switching model is for the ATEC charger. In order to use these results as pertaining to the actual unit itself, it would be necessary to analyze the fidelity of the simulation to the actual hardware which is built.

REFERENCES

[1] ANSI/NFPA 70-1990, National Electrical Code.

[2] "IEEE Recommended Practice for Electric Power Systems in Commercial Buildings," IEEE Std 241-1990, 18 Sep 1991.

[3] "SAE Electric Vehicle Conductive Charge Coupler," SAE Std J1772, November 2001.

[4] Electricity Information Administration, "U.S. Average Monthly Bill by Sector, Census Division, and State 2006," Electricity Information Administration, 2006. [Online]. Available: http://www.eia.doe.gov/cneaf/electricity/esr/table5.html.

[5] V. H. Johnson, "Battery performance models in ADVISOR," Journal of Power Sources, vol. 110, pp 321-329, 2002. [Online]. Available: www.elsevier.com/locate/jpowsour.

[6] P. T. Staats, W. M. Grady, A. Arapostathis, R. S. Thallam, "A Statistical Method for Predicting the Net Harmonic Currents Generated by a Concentration of Electric Vehicle Battery Chargers," IEEE Transactions on Power Delivery, vol. 12, no. 3, pp. 1258-1266, July 1997.

[7] Eaton Cutler-Hammer, "Medium Voltage Current Limiting Fuse Product Guide," *PG01303001E*, July 2003.

[8] Gomez, J. C.; Morcos, M. M., "Impact of EV Battery Chargers on the Power Quality of Distribution Systems," Power Engineering Review, IEEE , vol.22, no.10, pp.63-63, Oct. 2002

[9] "IEEE recommended practices and requirements for harmonic control in electrical power systems," IEEE Std 519-1992, 12 Apr 1993.

[10] "IEEE Recommended Practice for Establishing Liquid-Filled and Dry-Type Power and Distribution Transformer Capability When Supplying Nonsinusoidal Load Currents," IEEE Std C57.110-2008, 15 August 2008

APPENDIX

Figure A 1: Prototype Parking Deck

Voltage drop and Approximate Cost of Various Cable Sizes

Parameter	Value
Voltage	240 V
Voltage Drop	3.6 V
Spots	4
Lines	1
ft/spot	8.5714
Rating of Charger	7.68 kVA
Price of Cu	1.7305 USD/lb
Density of Cu	8.96 g/cm^3
Calc'd Length	10.45028571 meters
Calc'd Rating	**128 A per cable**

Ampacity at 75° C (A)	AWG	Area (kcmil)	Area (cm^2)	Diameter (cm)	Diameter (in)	Volume (cm^3)	Weight (lb)	Approximate Price	Cost per Spot	Z (Ω/1000 ft)	L_{max} (ft)*	L_{max} (m)*
14	18	1.62	0.0082	0.1024	0.0403	8.60	0.17	$0.2940	$0.07	-	-	-
18	16	2.58	0.0131	0.1291	0.0508	13.68	0.27	$0.4675	$0.12	-	-	-
20	14	4.11	0.0208	0.1628	0.0641	21.75	0.43	$0.7434	$0.19	2.7	10.42	3.18
25	12	6.53	0.0331	0.2053	0.0808	34.58	0.68	$1.1820	$0.30	1.7	16.54	5.04
35	10	10.38	0.0526	0.2588	0.1019	54.98	1.09	$1.8794	$0.47	1.1	25.57	7.79
50	8	16.51	0.0837	0.3264	0.1285	87.42	1.73	$2.9884	$0.75	0.69	40.76	12.42
65	6	26.25	0.1330	0.4115	0.1620	139.01	2.75	$4.7517	$1.19	0.45	62.50	19.05
85	4	41.74	0.2115	0.5189	0.2043	221.03	4.37	$7.5556	$1.89	0.29	96.98	29.56
100	3	52.63	0.2667	0.5827	0.2294	278.71	5.51	$9.5274	$2.38	0.24	117.19	35.72
115	2	66.37	0.3363	0.6544	0.2576	351.45	6.94	$12.0138	$3.00	0.19	148.03	45.12
130	1	83.69	0.4241	0.7348	0.2893	443.17	8.75	$15.1491	$3.79	0.16	175.78	53.58
150	1/0	105.53	0.5348	0.8251	0.3249	558.83	11.04	$19.1027	$4.78	0.13	216.35	65.94
175	2/0	133.08	0.6743	0.9266	0.3648	704.67	13.92	$24.0881	$6.02	0.11	255.68	77.93
200	3/0	167.81	0.8503	1.0405	0.4096	888.58	17.55	$30.3745	$7.59	0.092	305.71	93.18
230	4/0	211.60	1.0722	1.1684	0.4600	1120.47	22.13	$38.3015	$9.58	0.078	360.58	109.90
255	-	250.00	1.2668	1.2700	0.5000	1323.81	26.15	$45.2522	$11.31	0.07	401.79	122.46
285	-	300.00	1.5201	1.3912	0.5477	1588.57	31.38	$54.3026	$13.58	0.063	446.43	136.07
310	-	350.00	1.7735	1.5027	0.5916	1853.33	36.61	$63.3530	$15.84	0.058	484.91	147.80
335	-	400.00	2.0268	1.6064	0.6325	2118.10	41.84	$72.4035	$18.10	0.053	530.66	161.75
380	-	500.00	2.5335	1.7961	0.7071	2647.62	52.30	$90.5043	$22.63	0.048	585.94	178.59
420	-	600.00	3.0402	1.9675	0.7746	3177.14	62.76	$108.6052	$27.15	0.044	639.20	194.83
460	-	700.00	3.5470	2.1251	0.8367	3706.67	73.22	$126.7061	$31.68	0.04	703.13	214.31
475	-	750.00	3.8003	2.1997	0.8660	3971.43	78.45	$135.7565	$33.94	0.036	781.25	238.13
490	-	800.00	4.0537	2.2718	0.8944	4236.19	83.68	$144.8069	$36.20	-	-	-
520	-	900.00	4.5604	2.4097	0.9487	4765.71	94.14	$162.9078	$40.73	-	-	-
545	-	1000.00	5.0671	2.5400	1.0000	5295.24	104.60	$181.0087	$45.25	-	-	-
590	-	1250.00	6.3338	2.8398	1.1180	6619.05	130.75	$226.2608	$56.57	-	-	-
625	-	1500.00	7.6006	3.1109	1.2247	7942.86	156.90	$271.5130	$67.88	-	-	-
650	-	1750.00	8.8674	3.3601	1.3229	9266.67	183.05	$316.7652	$79.19	-	-	-
665	-	2000.00	10.1341	3.5921	1.4142	10590.48	209.20	$362.0173	$90.50	-	-	-

* Note: These calculations were done based on an aluminum conduit and 0.85 PF

Figure A 2: Cable Calculation Spreadsheet